The Environmental Toxin Arsenite Induces Tau Hyperphosphorylation†

Benoit I. Giasson,‡ Deepak M. Sampathu,‡ Christina A. Wilson,‡ Vanessa Vogelsberg-Ragaglia,‡ Walter E. Mushynski,§ and Virginia M.-Y. Lee*,‡

University of Pennsylvania School of Medicine, Third Floor Maloney Building, 3600 Spruce Street, Philadelphia, Pennsylvania 19104, and Department of Biochemistry, McGill University, 3655 Drummond, Room 914, Montreal, Quebec, H3G 1Y6

Received September 6, 2002; Revised Manuscript Received October 4, 2002

ABSTRACT: Abnormally hyperphosphorylated *tau* polymers known as paired helical filaments constitute one of the major characteristic lesions that lead to the demise of neurons in Alzheimer's disease. Here, we demonstrate that the environmental toxin arsenite causes a significant increase in the phosphorylation of several amino acid residues (Thr-181, Ser-202, Thr-205, Thr-231, Ser-262, Ser-356, Ser-396, and Ser-404) in *tau*, which are also hyperphosphorylated under pathological conditions. Complementary phosphopeptide mapping revealed a dramatic increase in the ^{32}P-labeling of many peptides in *tau* following arsenite treatment. Although arsenite activates extracellular-signal regulated kinases-1/-2 and stress-activated protein kinases, these enzymes did not contribute to the arsenite-increased phosphorylation, nor did they appear to normally modify *tau* in vivo. *Tau* phosphorylation induced by arsenite did not involve glycogen synthase kinase-3 or protein phosphatase-1 or -2, but the activity responsible for *tau* hyperphosphorylation could be inhibited with the protein kinase inhibitor roscovitine. The effects of arsenite on the phosphorylation of some *tau* mutations (ΔK280, V337M, and R406W) associated with frontal-temporal dementia with parkinsonism linked to chromosome 17 was analyzed. The unchallenged and arsenite-induced phosphorylation of some mutant proteins, especially R406W, was altered at several phosphorylation sites, indicating that these mutations can significantly affect the structure of *tau* in vivo. Although the major kinase(s) involved in aberrant *tau* phosphorylation remains elusive, these results indicate that environmental factors, such as arsenite, may be involved in the cascade leading to deregulation of *tau* function associated with neurodegeneration.

Alzheimer's disease (AD)[1] is a progressive neurodegenerative disease and constitutes the most common form of late onset dementia. It is characterized by neuronal loss and brain lesions in the form of senile plaques, neurofibrillary tangles (NFTs) and neuropil threads (*1*, *2*). The formation of these pathological markers may represent the aberrant regulation of cellular mechanisms that converge to lead to neuronal dysfunction and death. While the deposition of β-amyloid (Aβ) peptides characterizes senile plaques, paired helical filaments (PHFs), comprised of the hyperphosphorylated microtubule-associated protein *tau*, are the predominant structures in NFTs and neuropil threads (*1*, *2*). The identification of a spectrum of mutations in the *tau* gene in families with frontal-temporal dementia with parkinsonism linked to chromosome-17 (FTDP-17) that result in aberrant splicing and missense mutations [reviewed in ref *3*] demonstrates that alteration in *tau* function can be causal of disease.

PHF-*tau* in Alzheimer's disease brain is phosphorylated at 24 Ser or Thr amino acid residues (*4*, *5*). Ten of these sites, many of which are heavily phosphorylated (i.e., Ser-199, Ser-202, Thr-231, Ser-396, and Ser-404), are followed by a Pro. Numerous kinases have been shown to phosphorylate *tau* in vitro (see ref *6* for review), including stress-activated protein kinases (SAPKs) (*7*−*9*). SAPKs are members of the serine/threonine proline-directed kinase family known as mitogen-activated protein kinases (MAPKs)(see refs *10* and *11* for reviews). All MAPKs are activated by complex signal transduction pathways which include upstream MAPK kinase kinases and MAPK kinases (see refs *10* and *11* for reviews). The latter are dual-specificity MAPK kinases that phosphorylate the Thr-X-Tyr motif within the activation loop of MAPKs (*10*). MAPKs can be divided into three subgroups based on single amino acid residue differences within their activation loop. The first subgroup of MAPKs, the extracellular-signal regulated kinases (ERKs), have a Glu residue at the X position and are activated

† This work was supported by grants from the Canadian Institutes of Health Research (W.E.M.) and from the Alzheimer's Association and the National Institutes for Aging (V.M.-Y.L.). B.I.G. is the recipient of a fellowship from the Canadian Institutes of Health Research. V.M.-Y.L. is the John H. Ware 3rd Chair of Alzheimer's disease research of the University of Pennsylvania.

* Corresponding author. Address: Center for Neurodegenerative Disease Research, Department of Pathology and Laboratory Medicine, Maloney 3, HUP, Philadelphia, PA 19104-4283. Tel: 215-662-6427. Fax: 215-349-5909. E-mail: vmylee@mail.med.upenn.edu.

‡ University of Pennsylvania School of Medicine.

§ McGill University.

[1] Abrreviations: AD, Alzheimer's diseases; CHO, Chinese hamster ovary; ERK, extracellular-signal-regulated kinase; FTDP-17, frontal-temporal dementia with parkinsonism linked to chromosome 17; GSK, glycogen synthase kinase; MAPK, mitogen-activated protein kinase; MARK, microtubules/MAP-affinity regulating kinase; MBP, myelin basic protein; NFT, neurofibrillary tangles; OA, okadaic acid; PAO, phenylarsine oxide; PHF, paired helical filaments; PP, protein phosphatase; SAPK, stress-activated protein kinase.

10.1021/bi026813c CCC: $22.00
Published on Web 11/23/2002

predominantly by growth factors and growth stimuli. The ERK subgroup includes the well characterized ERK-1 and ERK-2 (*12*), as well as ERK-5 (*13*), for which less information is available. MAPKs with a Pro within the activation domain amino acid triplet are known as SAPK-1α, -1*β*, and -1*γ*, or cJun N-terminal kinase (JNK)-2, -3, and -1, respectively (*14*, *15*). The third subgroup of MAPKs include SAPK-2α/CSBP/p38α (*16*, *17*), SAPK-2*β*/p38−2/p38-*β*2 (*18*, *19*), SAPK-3/p38*γ*/ERK-6 (*20*−*22*), and SAPK-4/p38*δ* (*23*−*25*), all of which have a Gly residue at the X-position within the activation domain. In general, SAPKs are predominantly activated by cytokines and cellular stresses.

Arsenic is a common environmental element, especially in drinking water (*26*), but its levels are significantly increased by human activities (*27*). Environmental and occupational exposure to elevated concentrations of arsenic, which may result from smelting of other metals, coal combustion, and application of arsenical pesticides and herbicides, has been linked to an increased incidence of multiple forms of cancer and other diseases (*26*, *28*−*30*). It is well documented that acute exposure to arsenite can result in neuronal injury, especially in the form of peripheral axonopathy (*31*−*33*). However, arsenite can also impair central nervous system functions, as demonstrated by encephalopathy associated with headache, mental confusion, paranoia, and coma (*33*−*37*). Impairments in learning and memory were also reported and may be under-diagnosed (*38*, *39*). Arsenic exposure is generally in the form of two valence states, arsenate (As^{5+}), or arsenite (As^{3+}). Arsenite is thought to exert toxicity primarily by reacting with sulfhydryl groups and can potentially inhibit more than 200 enzymes (*40*), but it can also perturb cellular homeostasis by augmenting the levels of oxyradicals (*41*). Arsenite preferentially targets vicinal dithiols (*42*) such as lipoic acid, a cofactor of the pyruvate dehydrogenase multienzyme complex, resulting in a stable 6-membered ring and enzyme inactivation. Arsenite is an excellent chemical inducer of the heat-shock response (*43*) and a potent activator of SAPKs (*44*, *45*). Since SAPKs and environmental stressors have been implicated in modulating *tau* phosphorylation, we investigated the effects of arsenite on *tau* phosphorylation in vivo.

EXPERIMENTAL PROCEDURES

Materials. Carrier-free $^{32}P_I$ and [*γ*-^{32}P]-ATP were purchased from ICN Biomedicals (Mississisauga, ON). Enhanced chemiluminescence reagents were obtained from NEN (Mississauge, ON). Protein A-Sepharose was from Amersham Pharmacia Biotech (Piscataway, NJ). Anti-SAPK-1*γ* (C-17), anti-ERK-1 (C-16), and anti-ERK-2 (C-14) rabbit polyclonal antibodies as well as glutathione S-transferase (GST)-cJun (amino acids 1−79) were from Santa Cruz Biotechnology (Santa Cruz, CA). Myelin basic protein (MBP) was from Life Technologies Inc. (Burlington, ON). SB203580, kenpaullone, roscovitine, and olomoucine were obtained from Calbiochem Corp. (San Diego, CA). Okadaic acid (OA) was obtained from LC Services (Woburn, MA). Mouse anti-*tau* monoclonal antibodies AT8 and AT270 were from Innogenetics, Inc (Alpharetta, GA). Anti-JNK-1/-2 (G151−666) and anti-phospho-SAPK (Thr 183/Tyr 185) were from BD PharMingen Pharmagen (San Diego, CA) and New England Biolabs Inc (Beverly, MA), respectively.

Cell Culture. Chinese hamster ovary (CHO) T40 cells (a cell line stably expressing the longest isoform of human CNS *tau*, i.e., two N-terminal insert and four tandem repeats) (*46*, *47*) and cell lines expressing mutant *tau* proteins (*48*) were maintained in α-minimal essential medium, 10% fetal bovine serum (Life Technologies Inc., Burlington, ON), 100U/ml penicillin, 100U/ml streptomycin, and 200 *μ*g/mL Geneticin (Life Technologies, Rockville, MD). Neuro 2A and HEK 293 cells were obtained from the American Type Culture Collection (Rockville, MD) and cultured in Dulbecco's modification of Eagle's medium-high glucose 4.5 g/L, supplemented with 10% fetal bovine serum, 100U/ml penicillin, 100U/mL streptomycin, and 2 mM L-glutamine. These cells were transiently transfected using lipofectamine reagents (Life Technologies Inc., Burlington, ON) according to the manufacturer's instructions.

CHO T40 cells predominantly in interphase or mitosis were prepared as previously described (*49*). In short, CHO T40 cells were arrested in mitosis using 0.4 *μ*g/mL nocodazole for 8 h, mechanically separated (knocked-off) from nonsynchronized cells, and preplated with nocodazole for maintenance in mitosis. Using this method, approximately 90% of the nonsynchronized cells are in interphase.

Gel Electrophoresis and Western Blotting. Cells were harvested in phosphate-buffered saline (PBS) (137 mM NaCl, 2.7 mM KCl, 10 mM Na_2HPO_4, 1.8 mM KH_2PO_4), lysed in 2% SDS, 62.5 mM Tris, pH 6.8, and protein concentrations were determined using the bicinchoninic acid (BCA) assay (Pierce, Rockford, IL). The cell extracts were diluted to the appropriate concentrations with SDS−sample buffer (2% SDS, 62.5 mM Tris, pH 6.8, 10% glycerol and 5% *β*-mercaptoethanol), and the proteins were resolved on slab gels by SDS−polyacrylamide gel electrophoresis. Proteins were electrophoretically transferred to nitrocellulose membranes (Schleicher and Schuell, Keene, NH) in buffer containing 48 mM Tris, 39 mM glycine, and 10% methanol. Membranes were blocked with 5% skimmed milk powder dissolved in Tris-buffered saline−Tween (20 mM Tris (pH 7.7), 137 mM NaCl, and 0.1% Tween-20), incubated with primary antibodies followed by anti-mouse or anti-rabbit HRP conjugates antibodies, and visualized by enhanced chemiluminescence as described by the manufacturer.

^{32}P Metabolic Labeling and Phosphopeptide Mapping. Cells were incubated with 0.25 mCi of carrier-free ^{32}P/ml of P_i-reduced medium [19:1 of P_i-free Dulbecco's modification of Eagle's medium (Flow Laboratories, McLean, VA) to normal medium supplemented with 1% FBS] for 5 h before the addition of 500 *μ*M sodium arsenite for 2 h. Cells were harvested in PBS and lysed in detergent buffer (150 mM NaCl, 1% Nonidet-P40, 0.5% sodium deoxycholate, 0.1% SDS, 50 mM Tris, pH 8.0, 20 mM NaF, 2 mM EGTA, 0.5% levamisole, 1 mM $NaVO_4$, 1 mM PMSF, 25 *μ*M leupeptin and 40 units/ml aprotinin). Cellular debris were removed by centrifugation at 13 000*g* for 30 s, and 1% SDS was added to the supernatant. Samples were boiled for 5 min and diluted 10-fold in Triton buffer (1% Triton X-100, 50 mM Tris, pH 7.5, 100 mM NaCl, 2 mM EGTA, 2 mM levamisole, 50 mM NaF, 1 mM PMSF, 25 *μ*M leupeptin, and 40 units/ml aprotinin). *Tau* was immunoprecipitated for 3 h at 4 °C with protein A-Sepharose preabsorbed with antibody 17026, a rabbit polyserum raised to full-length recombinant *tau* (*66*). The immunoprecipitates were washed

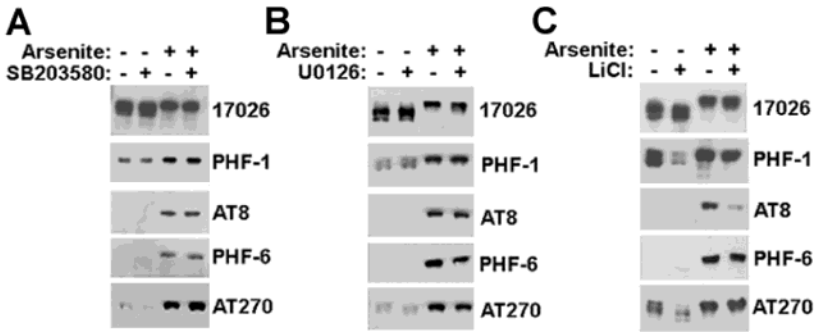

FIGURE 1: Arsenite induces *tau* phosphorylation in CHO T40 cells. Western blot analysis of CHO T40 cells pretreated with 20 μM SB 203580 (A), 10 μM U0126 (B), or 10 mM LiCl for 1 h (C) before the addition of 500 μM arsenite for 2 h. Five μg of total cell lysate was loaded on each well of 10% polyacrylamide gels.

repeatedly with Triton buffer and eluted by boiling for 5 min in SDS sample buffer.

Following immunoprecipitation, metabolically ^{32}P-labeled *tau* was resolved by SDS−PAGE, visualized by autoradiography and excised from the gel. The gel slices were washed with 20% methanol, lyophilized, and digested for 18 h at 37 °C in 50 mM ammonium bicarbonate containing 10 μg/mL of N$^{\alpha}$-p-tosyl-L-lysine chloroketone-treated α-chymotrypsin (Sigma, Chemicals Co., St. Louis, MO). After the gel slices were removed, peptides were lyophilized, dissolved in H_2O and loaded onto cellulose thin-layer chromatography sheets (MN-300; EM Science, Griggstown, NJ). Phosphopeptides were resolved as described (*50*) and were visualized by autoradiography.

Immunoprecipitation Kinase Assays. SAPK-1γ activity was assayed as described previously (*45*). In short, after cell lysis in the presence of Triton X-100, cell debris was removed by centrifugation at 13 000*g*, and the protein concentration of each supernatant was determined to equalize the amount used in each immunoprecipitation. SAPK-1γ was immunoprecipitated, the immunoprecipitates were washed extensively, and activity was assayed using [γ-^{32}P]ATP and GST-cJun as a substrate. After stopping the reaction with SDS−sample buffer, GST-cJun was resolved on 10% polyacrylamide gels. The gels were stained with Coomassie Blue R-250, destained with 10% 2-propanol/10% acetic acid followed by 50% methanol/5% glycerol, dried, and exposed to a PhosphorImager plate. The radioactive signal was quantified using ImageQuant software (Molecular Dynamics, Inc., Sunnyvale, CA).

ERK-1/-2 activity was also assayed as described previously (*45*). The procedure was similar to SAPK-1γ imunoprecipitation kinase assays, except antibodies specific for ERK-1 and ERK-2 were used from the immunoprecipitation and MBP was used as the substrate. GSK-3 activity was measured as previously described (*61*).

Infection of CHO T40 Cells with Semliki Forest Virus (SFV). Using polymerase chain reaction (PCR) engineering and specific oligonucleotides, an amino-terminal HA tag (MYPYDVPYA) and Bam HI restriction sites were added to the human SAPK-1γ cDNA. Using PCR, the human SAPKK-1 cDNA was modified with an amino-terminal Myc-tag (MAEQKLISEEDLN), a 5′ end AvrII restriction site, and a 3′end Cla I restriction site. These modified cDNAs were cloned in the dual promoter SFV-based vector pSFVdPG-X (*51*). SFV virus was prepared and titered in BHK cells as previously described (*52*). Cells were infected in serum-free medium at a multiplicity of infection of approximately 10. One hour after infection, the medium was replaced with complete medium, and cells were harvested after 24 h.

In-Gel Kinase Assay. Cell extracts (15 μg) in SDS−sample buffer were resolved on 9% polyacrylamide gels polymerized in the presence of 250 μg/mL recombinant human T40 *tau* isoform, 250 μg/mL MBP, or no protein (as a control). Following electrophoresis, gels were washed with 20% 2-propanol, 50 mM Tris, pH 8.0, to remove SDS. Proteins were denatured by incubating the gels in 50 mM Tris, pH 8.0, 5 mM β-mercaptoethanol for 1 h, followed by 50 mM Tris, pH 8.0, 6 M guanidine-HCl, 20 mM DTT, 2 mM EDTA for 1 h. Gels were incubated in 50 mM Tris, pH 8.0, 1mM DTT, 2 mM EDTA, 0.04% Tween 20 overnight at 4 °C to allow proteins to renature. Gels were equilibrated in 40 mM Hepes, pH 8.0, 1 mM DTT, 0.1 mM EGTA, 20 mM $MgCl_2$, 100 uM vanadate for 1 h, and the kinase reaction was carried out in the same buffer containing 30uM ATP (10 uCi/ml) for 1 h at room temperature with gentle shaking. The reaction was stopped by fixing gels with 10% 2-propanol/10% acetic acid, followed by 50% methanol/5% glycerol. After drying the gels, protein kinase bands were detected by exposing the gels to a PhosphorImager plate.

Cell-Free Kinase Assay. CHO T40 cells were grown to ∼40% confluency and pretreated with or without 200 μM roscovitine for 1 h, followed by treatment with or without 500 μM sodium arsenite for 1.5 h. Cells were scraped in PBS and lysed by sonication in 50 mM Tris pH 7.5, 2mM EDTA containing a cocktail of protease inhibitors. Cell debris was removed by centrifugation at 4000*g* for 5 min at 4 °C. In vitro kinase assays were conducted by adding 10 mM $MgCl_2$, 1 mM ATP, and 5 μCi γ^{32}P-ATP with or without 0.25 mg/mL recombinant *tau* T40 to the cell lysates followed by incubation at 37 °C for 30 min. Kinase reactions were terminated by adding SDS−sample buffer and heating at 95 °C for 5 min. Samples were subjected to 10% SDS−PAGE, followed by autoradiography and visualized using a Phosphorimager.

RESULTS

Antibody 17026, a rabbit antiserum raised against full-length recombinant *tau*, was used to detect all isoforms of *tau*. Challenging CHO T40 cells with 500 μM arsenite for 2 h resulted in a reduction in the mobility of *tau* on SDS−PAGE (Figure 1), suggestive of an increase in phosphorylation (*53*, *54*). Increased phosphorylation was directly

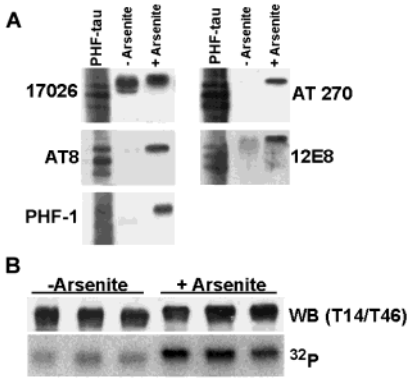

FIGURE 2: Analysis of the increase in *tau* phosphorylation in arsenite-treated cells. (A) Western blot analysis of the level of *tau* phosphorylation in arsenite-treated CHO T40 cells compared to PHF-*tau*. Approximately equal amounts of PHF-*tau* and *tau* in CHO T40 cells extracts were subject to this analysis, as demonstrated using the polyclonal antibody 17026. The levels of *tau* phosphorylation in CHO T40 cells challenged with 500 μM arsenite for 2 h (+ arsenite) was comparable to PHF-*tau* at the AT8, PHF-1, AT270, and 12E8 phospho-epitopes. (B) Determination of the relative increase in *tau* phosphorylation induced by arsenite treatment. CHO T40 cells were preincubated with ^{32}Pi and left untreated (− arsenite) or treated with 500 μM arsenite (+ arsenite) for 2h. *Tau* was immuno-precipitated as described in Experimental Procedures and visualized by Western blotting using the phosphorylation-independent antibodies T14 and T46. After Western blotting, the membrane was rinsed with water, dried and ^{32}P-labeled *tau* was detected by exposing to a PhosphoImager plate.

ascertained with several monoclonal antibodies that recognize phosphorylation dependent epitopes. The immunoreactivities to PHF-1 (specific for phosphoserine 396/404) (*55*), PHF-6 (specific to phosphoserine 231)(*56*), AT8 (specific to phosphoserine 202 and phosphothreonine 205) (*57*), and AT270 (specific to phosphoserine 181) (*58*) were increased due to arsenite treatment. Similar results were obtained when cells were challenged with 50 μM arsenite for 6−10 h (data not shown).

The increase in *tau* phosphorylation induced by arsenite was compared to the levels of phosphorylation in PHF-*tau* biochemically purified from AD brain (*53*). These experiments were normalized with the antibody 17026 so that approximately equivalent amounts of *tau* are present in preparations of PHF-*tau* compared to CHO T40 cells extracts (Figure 2A). The level of *tau* phosphorylation in arsenite-treated CHO T40 cells was similar to that of PHF-*tau* at the AT8, PHF-1, and AT270 sites (Figure 2A). The level of PHF-6 immunoreactivity was much lower in arsenite-treated cells compared to that in PHF-*tau* (data not shown). The effect of arsenite treatment on the 12E8 epitope, which recognizes the nonproline directed phosphorylation sites Ser 262/Ser356 (*90*), was also evaluated and compared to PHF-*tau*. Arsenite also induced an increase in the phosphorylation of this site that was comparable to the phosphorylation state in PHF-*tau*.

The relative increase in total *tau* phosphorylation was analyzed by labeling CHO T40 cells with ^{32}Pi and immunoprecitating equivalent amounts of *tau* from CHO T40 cells under control conditions or after treatment with arsenite. These experiments are depicted in triplicate in Figure 2B. The levels of immunoprecipitated *tau* from CHO T40 cells were monitored using a mixture of phosphorylation-independent monoclonal antibodies T14 and T46 to minimize the immunodetection of the rabbit IgG used for immunoprecipitation with the secondary antibody used for Western blotting. Relative overall phosphorylation of *tau* was 4.5-fold ± 0.9 greater in arsenite-treated cells compared to untreated cells.

To assess the overall effect of arsenite on protein phosphorylation, triplicate lysates of cells labeled with ^{32}Pi and left untreated or challenged with 500 μM arsenite were separated by SDS−PAGE, transferred onto a nitrocellulose membrane, and analyzed by autoradiography. Arsenite treatment did not result in an overall increase in protein phosphorylation, although there were some differences in the intensity of some phospho-protein bands (Figure 3A). Interestingly, there was a significant increase in phosphate incorporation in a protein band (~70 kD) with mobility on SDS−PAGE consistent with that of T40 *tau.* Immunoblotting for *tau* using the nitrocellulose membrane used for the determination of the relative levels of protein phosphorylation demonstrated a reduction in the mobility of *tau* resulting from arsenite treatment (Figure 3B). Furthermore, the ~70 kD band identified by a triangle in Figure 3A overlapped exactly with the *tau* band identified by Western blotting in the samples from cells treated with arsenite (Figure 3B). To further confirm that this phospho-protein band was *tau*, ^{32}P-labeling of proteins in CHO and CHO T40 cells was compared with or without arsenite treatment (Figure 3C). The phospho-protein band in CHO T40 cells, identified by a triangle, was not present in CHO cells, indicating that this phosphorylated protein is *tau*.

The analysis of overall protein phosphorylation demonstrated that arsenite did not have an overwhelming effect on cellular metabolism. To further ascertain the effect of arsenite on cellular physiology, cell viability was determined by trypan blue exclusion assay. Treatment with 500 μM arsenite did not have an immediate effect on cell viability (trypan blue exclusion: untreated cells = 98.6% ± 0.5, arsenite treated cells = 97.2% ± 1.6, n = 6). Four hours after arsenite challenge, there still was no change in cell viability (trypan blue exclusion: untreated cells = 99.0% ± 1.2, arsenite treated cells = 99.6% ± 0.5, n = 6), but 24 h after arsenite treatment, the demise of a subpopulation of cells was observed (trypan blue exclusion: untreated cells = 98.6% ± 0.5, arsenite treated cell = 65.2% ± 7.8, n = 6). These results show that arsenite exposure did not completely obliterate cellular metabolism and the delay in cell death may be due to arsenite inducing apoptotic mechanisms (*95*), although the occurrence of this type of changes in arsenite treated CHO cells will require further studies.

Since analyzing changes in *tau* phosphorylation by using phosphorylation-dependent antibodies is limited to sites for which antibodies are available, phosphopeptide mapping analysis was conducted to provide a more complete index of the phosphorylation profile of *tau* in CHO T40 cells. Phosphopeptide mapping revealed that arsenite treatment caused the accretion of phosphate on numerous amino acid residues in *tau*. In untreated cells, *tau* is phosphorylated at one major site (phosphopeptide 4) and a few minor sites (Figure 4A). The addition of arsenite caused a dramatic increase in the phosphorylation of many sites, marked by numbers or asterisks (Figure 4B).

Most MAPKs are activated by arsenite treatment, which complicates the identity of the enzyme(s) involved in *tau*

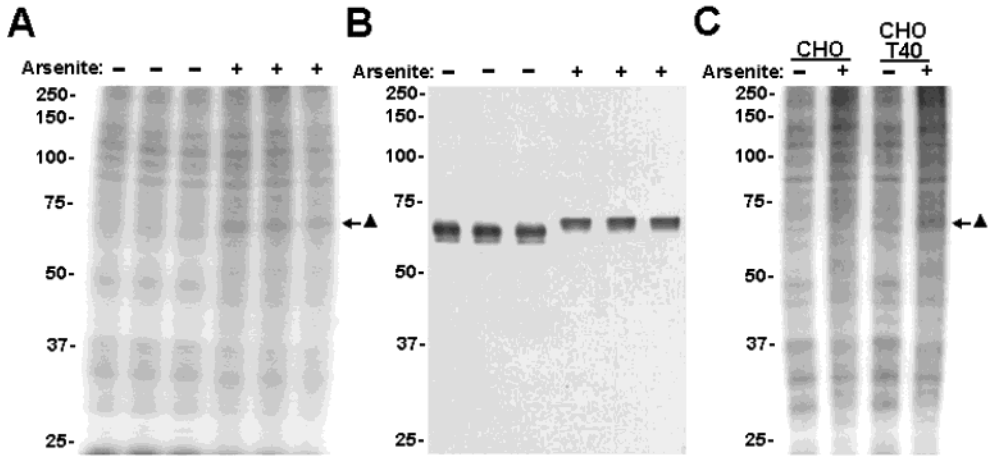

FIGURE 3: Identification of *tau* as a major subtract for arsenite-induced phosphorylation. (A) CHO T40 cells were preincubated with ^{32}Pi and left untreated (−) or treated with 500 μM arsenite (+) for 2h. Cells were washed with PBS and lysed in detergent buffer. Following the removal of cell debris by centrifugation, 5 μg of cell lysates was loaded on separate wells of a 9% SDS−polyacrylamide gel. Proteins were transferred electrophoretically to a nitrocellulose membrane that was exposed to a PhosphoImager Plate. A ~70 kD phospho-protein band induced by arsenite is identified with a triangle. (B) The same nitrocellulose membrane as in panel A was probed with the anti-*tau* antibody 17026 and Western blotting analysis was performed as described in Experimental Procedures. (C) CHO and CHO T40 cells were preincubated with ^{32}Pi and left untreated (−) or treated with 500 μM arsenite (+) for 2 h. Cells were washed with PBS and lysed in detergent buffer. Following the removal of cell debris by centrifugation, 5 μg of cell lysates was loaded on separate wells of a 9% SDS−polyacrylamide gel. The gel was fixed, dried, and exposed to a PhosphoImager Plate. The phospho-protein band that demonstrates increased phosphorylation following arsenite treatment (identified with a triangle) was present in CHO T40 cells, but not in CHO cells. The mobility of molecular mass markers is depicted on the left of each panel.

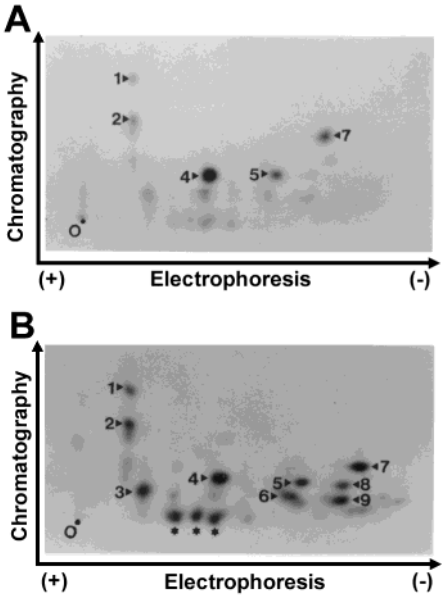

FIGURE 4: Two-dimensional phosphopeptide mapping of *tau* from CHO T40 cells. CHO T40 cells were preincubated with ^{32}Pi and left untreated (A) or treated with 500 μM arsenite for 2 h (B). O represents the origin where the peptides were spotted. The phosphopeptides labeled with numbers from 1 to 9 or stars (*) represent the major sites labeled with ^{32}Pi.

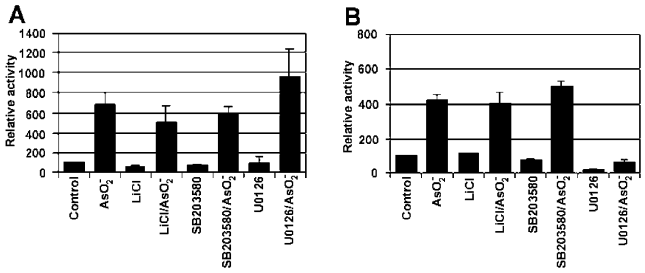

FIGURE 5: Activation of SAPK-1γ and ERK-1/-2 by arsenite. (A) Immunoprecipitation kinase assays of SAPK-1γ and (B) ERK-1/-2 in T40 CHO cells following the addition of 500 μM arsenite for 2 h. Cell were challenged with LiCl (10 mM), SB 203580 (20 μM), or U0126 (10 μM) for 3 h total or 1 h prior to the addition of arsenite. Kinase activities were assayed as described in Material and Methods. $N = 3$.

phosphorylation under arsenite stress. The involvement of some of these enzymes such as SAPK-2α/β and ERK-1/2, which can phosphorylate *tau* in vitro, can be readily ascertained with specific inhibitors. SB203580 is a specific inhibitor of SAPK-2α/β (*25*, *59*), while the compound U0126 (1,4-diamino-2,3-dicyano-1,4-bis[2-aminophenylthio]butadiene) specifically blocks ERK-1/-2 activity by inhibiting the direct upstream activator MAP kinase kinases, MEK-1 and MEK-2 (*60*). Neither compound reduced the normal levels of *tau* phosphorylation or prevented arsenite-induced phosphorylation (Figs. 1A and B). GSK-3, also a proline-directed kinase, is the most well-documented kinase involved in *tau* phosphorylation in vivo (*61*). Although there is no evidence for the induction of GSK-3 by arsenite, the involvement of this kinase was analyzed with the inhibitor LiCl. Treatment with LiCl reduced the steady-state levels of PHF-1 and AT270, consistent with the notion that GSK-3 is constitutively active and normally involved in *tau* phosphorylation (*61*). LiCl did not block the increase in PHF-1, PHF-6 or AT270 immunoreactivity, but it did reduce the increase in AT8 immunoreactivity. Arsenite treatment resulted in a slight increase in GSK-3 activity (1.5-fold $\pm$ 0.4; $n = 4$) as measured by immunoprecipitation kinase assay (*61*).

SAPK-1γ- and ERK-1/2 immunoprecipitation kinase assays were conducted to verify that arsenite induces MAPK activities in CHO T40 cells and to validate the efficacy and specificity of the kinase inhibitors. Addition of arsenite resulted in approximately 7-fold increase in SAPK-1γ activity (Figure 5A) and 4-fold increase in ERK-1/-2 activity (Figure 5B). Pretreatment with LiCl or SB203580 did not affect SAPK-1 γ activity, but U0126 slightly augmented the effect of arsenite. U0126 inhibited the basal ERK-1/2 activity

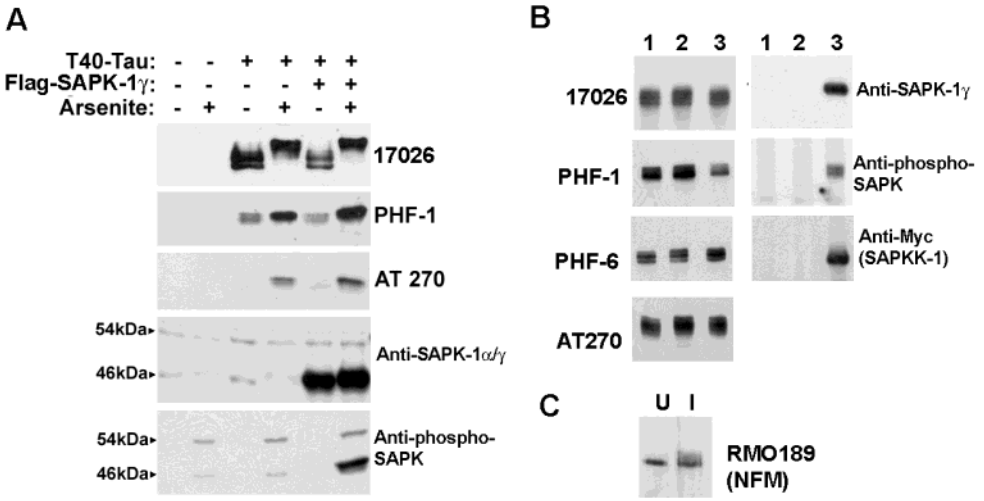

FIGURE 6: Overexpression and activation of SAPK-1 does not coincide with *tau* phosphorylation in vivo. (A) Western blot analyses of HEK 293 cells transiently transfected with vectors expressing Flag-SAPK-1γ and/or T40 *tau* and challenged with 500 μM arsenite for 2 h. (B) CHO T40 cells were uninfected (lane 1) or infected with SFV/LacZ (lane 2) and SFV/SAPK-1 γ-SAPKK-1 (lane 3). *Tau*, SAPK-1γ, and SAPKK-1 expression and phosphorylation were determined by Western blot analysis. A 5 μg sample of total protein lysate was added in each lane of 10% polyacrylamide gels. (C) NT2N cells were uninfected (U) or infected with SFV/SAKP-1γ-SAPKK-1, and 10 μg of total cell lysate was loaded on a 6% polyacrylamide gel followed by Western blotting analysis with antibody RMO189.

and blocked the arsenite-induced activity. LiCl did not affect ERK-1/-2 activity, but SB 203580 enhanced the arsenite-induced ERK activity slightly.

To investigate the involvement of SAPK-1 in the phosphorylation of *tau* in vivo, the SAPK-1 γ isoform was overexpressed in cells expressing *tau* (Figure 6A). HEK 293 cells were used for transient transfection, since they demonstrate a much greater transfectabilty than CHO cells. *Tau* was detected in these cells only after transfection with the expression vector T40-*tau* PSG5. The addition of arsenite to HEK 293 cells also induced a similar increase in phosphorylation, as evidenced by a reduction in electrophoretic mobility and increased PHF-1 and AT270 immunoreactivities. The 46 kDa and 54 kDa SAPK-1 isoforms are normally expressed in HEK 293 cells, but cotransfection with a plasmid expressing Flag-SAPK-1γ (*14*) resulted in a large increase in the amount of this enzyme. Addition of arsenite resulted in activation of SAPK-1, as indicated by its phosphorylation. However, the activation of this enzyme by arsenite, even when highly overexpressed, only slightly increased the phosphorylation of *tau*, indicating that *tau* is a poor substrate in vivo and that SAPK-1 is not involved in arsenite-induced phosphorylation.

The ability of SAPK-1γ to modify *tau* in vivo was further assayed by infecting CHO T40 cells with SFV/SAPK-1γ-SAPKK-1 (Figure 6B). Infection with this virus or the control virus SFV/LacZ did not increase the phosphorylation of *tau*. On the contrary, the phosphorylation of the PHF-1 epitope was reduced by infection with SFV/SAPK-1γ-SAPKK-1. The high levels of expression of SAPK-1γ and SAPKK-1 was demonstrated with an antibody specific to SAPK-1γ and the anti-Myc antibody 9E10, respectively. The activation of SAPK-1γ was monitored with the anti-phospho-SAPK-1 antibody. Furthermore, the ability of the SFV-expressed SAPK-1γ to phosphorylate a known substrate, such as the KSP-rich neurofilament subunits (*45*), was verified by infecting NT2N cells. The increased phosphorylation of the mid-size neurofilament subunit (NFM) was demonstrated by a reduction in electrophoretic mobility (Figure 6C).

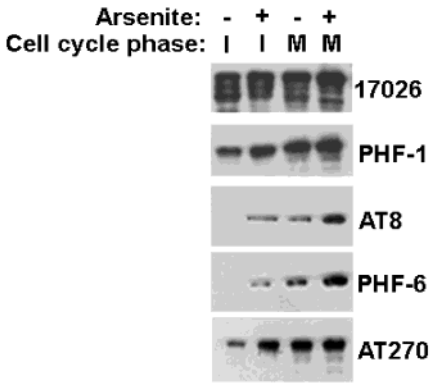

FIGURE 7: Arsenite induces *tau* phosphorylation during interphase and mitosis. CHO T40 cells were synchronized in either interphase or mitosis followed by the addition of 500 μM arsenite for 2 h. A 5 μg sample of total protein lysate was added in each lane of 10% polyacrylamide gels, and phosphorylation was monitored by Western blot analysis.

Arsenite can induce mitotic arrest in various cell lines (*62*−*64*), suggesting that cyclin-dependent proline-directed kinases may be involved in *tau* hyperphosphorylation. Further, previous studies have shown that *tau* becomes hyperphosphorylated during mitosis in CHO T40 cells as well as in other cell lines (*49*, *65*). To determine if arsenite-induced phosphorylation was due to cell cycle arrest, the effect of arsenite on cells in interphase and mitosis was studied. Mitotic cells demonstrated highly phosphorylated *tau* compared to cells in interphase, but arsenite treatment induced *tau* phosphorylation in both phases of the cell cycle, indicating that arsenite-induced *tau* phosphorylation is not merely due to cell cycle arrest (Figure 7).

To further characterize the arsenite-induced enzymatic activity responsible for *tau* phosphorylation, we used several previously described inhibitors of proline-directed kinases (Table 1). Treatment with 10 μM kenpaullone reduced the normal phosphorylation of *tau* at the PHF-1 and AT270 phosphorylation sites, but it did not affect the arsenite-induced phosphorylation at these sites (Figure 8A). There was a slight reduction in the arsenite-induced phosphorylation

Table 1: Summary of the Specificity of the Inhibitors of Proline-Directed Kinases

kinases	inhibitors IC_{50} (μM) kenpaullone	roscovitine	olomoucine	refs
cdk1/cyclin B	0.4	0.65	7	*86, 87, 88*
cdk2/cyclin A	0.68	0.7	7	*86, 88*
cdk2/cyclin E	7.5	0.7	7	*86, 88*
cdk4/cyclin D1	>100	>100	>1000	*86, 88*
cdk5/p35	0.85	0.16	3	*86, 87, 88*
cdk6/cyclin D3	N/A	>100	>250	*86, 88*
ERK-1	20	34	50	*86, 88*
ERK-2	9	14	40	*86, 88*
GSK-3β	0.23	220	130	*86, 87, 88*

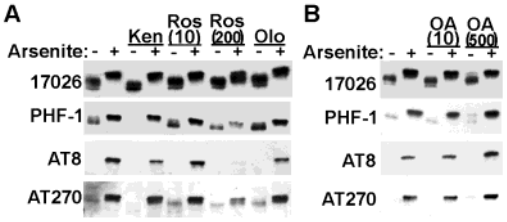

FIGURE 8: Characterization of arsenite-induced phosphorylation of *tau* in CHO T40 cells using protein kinase and phosphatase inhibitors. Western blot analysis of CHO T40 cells pretreated for 1 h (A) with kinase inhibitors [10 μM kenpaullone (Ken), 10 μM or 200 μM roscovitine (Ros), or 10 μM 200 μM olomoucine] or (B) the phosphatase inhibitor OA (10 or 500 nM). Cells were untreated (−) or challenged with 500 μM arsenite (+) for 2 h. A 5 μg sample for total cell lysate was loaded in each well of 10% polyacrylamide gels.

of the AT8 epitope. Ten μM roscovitine or 200 μM olomoucine did not reduce the levels of *tau* phosphorylation under unstimulated conditions, nor did they affect the increased phosphorylation resulting from arsenite exposure. However, higher concentration of roscovitine (200 μM) inhibited the arsenite-induced phosphorylation of *tau*, but without affecting the normal phosphorylation state.

Phosphatases, in particular protein phophatase (PP)-1 and-2A (*6*), are important enzymes involved in the regulation of the levels of *tau* phosphorylation. To investigate the involvement of these enzymes in the arsenite-induced *tau* phosphorylation, the effect of arsenite was compared to that of OA, a specific inhibitor of PP-1 (IC_{50} = 0.1−2 nM) and PP-2A (IC_{50} = 20−60 nM) (*83*, *84*). The addition of 10 nM OA had little effect on the phosphorylation state of *tau* with or without arsenite treatment (Figure 8B). Treatment with 500 nM OA had a slight effect on the phosphorylation of *tau* resulting from arsenite exposure, but the increase in levels of phosphorylation induced by arsenite alone was substantially more dramatic than the effects of OA alone.

In-gel kinase assays, using either MBP as a general kinase substrate or T40 *tau*, were used in an attempt to identify the kinase involved in *tau* phosphorylation following arsenite treatment (Figure 9). When the assay was performed with no protein substrate polymerized in the gel, no major bands were detected. In gels polymerized with MBP, a major ~40 kDa protein kinase activity was observed, which corresponds to ERK-1/-2. Using the in-gel kinase assay, we demonstrated ~2-fold increased in ERK activity, which is less sensitive than the immuno-precipitation kinase assay (Figure 5B). The use of *tau* as the substrate for the in-gel kinase assay revealed a protein kinase doublet at ~100 kDa. These bands have been shown to correspond to the microtubules/MAP-affinity

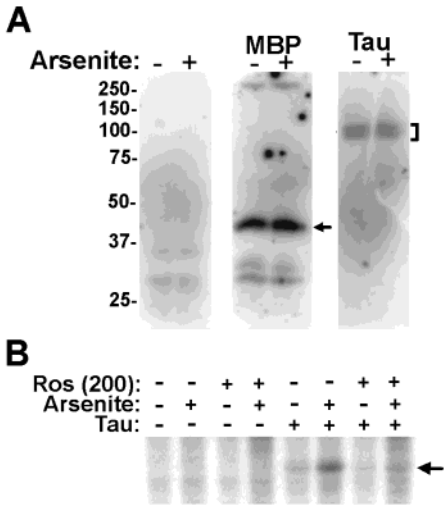

FIGURE 9: In-gel kinase assay and cell-free assay of kinase activites induced by arsenite. (A) The in-gel kinase assays were performed as described in Experimental Procedures. Cell extracts from untreated (−) or cells treated with 500 μM arsenite for 2 h (+) were resolved by SDS−PAGE. Polyacrylamide gels were polymerized without any protein, or in the presence of MBP or T40 *tau*. The arrow on the left indicates the position of the major MBP kinase. The bracket on the right indicates the position of the major T40 *tau* kinase. The mobilities of molecular mass markers are depicted on the right. (B) *Tau* kinase activity(ies) activated by arsenite was analyzed in a cell-free assay as described in Experimental Procedures. Assays were conducted in the absence (−) or presence (+) of recombinant human *tau* T40 in kinase buffer as indicated above the lanes. CHO cells were untreated or challenged with 500 μM arsenite. In some samples, cells were pretreated with 200 μM roscovitine. Following the kinase reaction, samples were resolved on 10% SDS−polyacrylamide gels. Gels were stained with Coomassie, destained, dried, and exposed to a PhosphoImager plate. The arrow indicates the band corresponding to *tau* T40.

regulating kinases-1 and -2 (*85*), but there was no increase in this activity in cells treated with arsenite.

To begin characterization of the enzymatic activity involved in the arsenite-induced phosphorylation of *tau*, we sought to determine if this activity(ies) could be monitored after cell lysis. In a cell-free assay, the phosphorylation of *tau* was significantly greater in extracts from cells treated with arsenite (Figure 9B). Furthermore, in a similar manner as intact cells, the increased phosphorylation of *tau* was partially inhibited with roscovitine.

It was recently demonstrated that treatment of cultured cells with the arsenic related compound phenylarsine oxide (PAO) could induce phosphorylation of *tau* at the 12E8 phospho-epitope (*91*, *92*). Since it is possible that arsenite and PAO may have a similar mode of action, the effect of each compound on the phosphorylation of *tau* in CHO T40 cells was compared using the previously described conditions for PAO (*91*). In a similar manner as arsenite, PAO treatment induced the phosphorylation of all sites analyzed by Western blotting using phospho-specific antibodies, albeit at a lower level (Figure 10). Furthermore, the effect of PAO could also be inhibited with roscovitine. It also was previously demonstrated that the PAO-induced phosphorylation of at least some sites in *tau* could be inhibited with the kinase inhibitor staurosporine (*91*). However, the addition of staurosporine (even at higher concentrations than previously described) did not inhibit the phosphorylation of *tau* induced by arsenite (Figure 11).

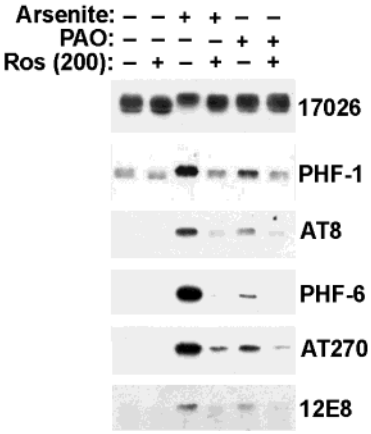

FIGURE 10: Comparison of effects of arsenite and PAO on *tau* phosphorylation in CHO T40 cells. Cells were untreated (−), treated with 500 μM arsenite for 2 h (+), or treated with 5 μM PAO for 45 min (+) as previously described (*91*). In some cases as indicated above the lanes, cells were pretreated with 200 μM roscovitine (Ros) for 1 h. *Tau* phosphorylation was monitored by Western blotting analysis.

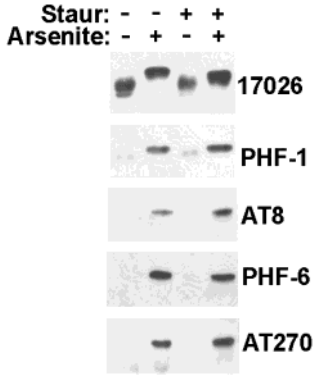

FIGURE 11: Staurosporine did not inhibit the arsenite-induced phosphorylation of *tau* in CHO T40 cells. Western blot analysis of CHO T40 cells pretreated for 1 h with 20 nM staurosporine (staur) and left unchallenged (−) or challenged with 500 μM arsenite (+) for 2 h. A 5 μg sample for total cell lysate was loaded in each well of 10% polyacrylamide gels.

The increase in phosphorylation of *tau* resulting from arsenite was demonstrated in two different cell types, HEK 293 and CHO cells. In addition, to determine the effect of arsenite on a neuronal cell line, Neuro 2A cells were exposed to arsenite. Arsenite challenge also resulted in increased phosphorylation of *tau* in these cells (Figure 12).

An increasing number of mutations in *tau* have been linked to FTDP-17. Many of these mutations affect the ability of *tau* to bind to microtubules (*66*), and recently it has been shown that mutations can have long-range effects on phosphorylation sites in vitro (*67*). To investigate the latter effect in vivo, CHO cells expressing wild-type and mutant T40 *tau* proteins were challenged with arsenite (Figure 13). Following arsenite treatment, a similar increase in PHF-1 immunoreactivity was observed for all *tau* proteins. Arsenite also increased the phosphorylation of all proteins at the AT270 epitope, but the increase was less for R406W. The V337M/P301L/R406W (VPR) triplet mutant protein exhibited an overall hypophosphorylation state in untreated cells as revealed by its relatively greater mobility on SDS−PAGE. The AT270 and PHF-6 epitopes, however, were more reactive, indicative of more pronounced phosphorylation at

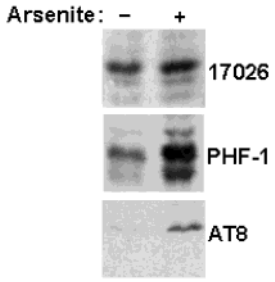

FIGURE 12: Arsenite-treatment induced the phosphorylation of tau in Neuro 2A cells. Neuro 2A cells were untreated (−) or challenged with 500 μM arsenite (+) for 2 h. The phosphorylation state of *tau* was monitored using antibodies that cross-react with murine *tau*. A 20 μg sample of total cell lysate was loaded in each well of 10% polyacrylamide gels.

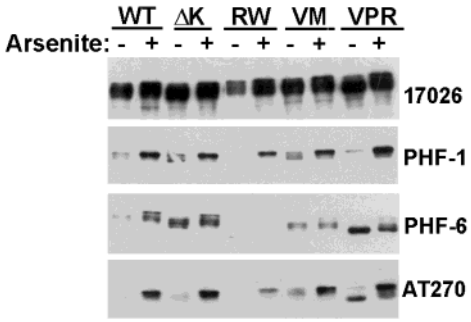

FIGURE 13: Effect of *tau* mutations on the induction of phosphorylation by arsenite. CHO cells expressing wild-type T40 *tau*, the single T40 *tau* mutants ΔK280 (ΔK), R406W (RW), V337M (VM), and the triple T40 *tau* mutant V337M/P301L/R406W (VPR) were challenged with 500 μM arsenite for 2 h. A 5 μg sample of total protein extract was loaded on 10% polyacrylamide gels, followed by Western blotting analysis.

Ser-181 and Ser-231, respectively. Arsenite treatment decreased the mobility of the VPR *tau* protein, which was especially noticeable with AT270. Although arsenite treatment increased the immunoreactivity for PHF-6 in the wild-type protein, there was no such increase for any of the mutant proteins, and the most pronounced paucity of phosphorylation of this site was for the R406W mutant.

DISCUSSION

We have demonstrated that exposure to the heavy metal arsenite results in a substantial increase in *tau* phosphorylation at many of the sites that are hyperphosphorylated in PHF-*tau* (Figures 1 and 2). Exposure to arsenite increased the overall phosphorylation of *tau* more than 4-fold, and it was shown that *tau* is a major substrate for the enzymatic activities that are affected by arsenite (Figure 3). Arsenite challenge elevated the phosphorylation level of several specific sites, including Ser-396/Ser-404, Thr-181, Ser-202/Thr-205, and Ser-262/Ser-356, to that of PHF-*tau* isolated from AD brain. Furthermore, it also promoted the phosphorylation of many additional sites that could not be monitored by the use of antibodies to phospho-specific epitopes (Figure 4), suggesting that arsenite exposure may closely recapitulate the phosphorylation state found in PHF-*tau*.

Increased *tau* phosphorylation was not due to SAPK-2α/β or ERK-1/2 activation, and these enzymes do not seem to phosphorylate *tau* in vivo (Figure 1A and B). For example, inhibition of constitutive or arsenite-induced ERK-1/2 activity

(Figure 1B and 5B) did not affect the phosphorylation state of *tau*. These results underscore the need to be cautious with in vitro data, since in the latter setting *tau* can be a substrate for ERKs (*68*, *69*). Our data are consistent with reports demonstrating that in vivo activation of ERKs resulted in only a slight increase in *tau* phosphorylation without any detectable changes in phospho-dependent epitope immunoreactivity (*70*, *71*).

Although GSK-3 is a major kinase modulating the phosphorylation of *tau* in vivo (*61*), as exemplified by the reduction in the immunoreactivity of PHF-1 and AT270 by LiCl (Figure 1C) and kenpaullone (Figure 8A), it is not involved in the arsenite-induced phosphorylation of *tau*. Neither LiCl nor kenpaullone inhibited the increased phosphorylation at sites detected by AT270, PHF-1, or PHF-6 following arsenite treatment. The increase in AT8 phosphoepitope immunoreactivity due to arsenite was diminished by LiCl and kenpaullone, suggesting that GSK-3 and the arsenite-induced kinase(s) may have an additive role in modifying this epitope.

Tau, which can be phosphorylated by SAPK-1s in vitro (*8*, *9*), also does not appear to be a substrate for these enzymes in vivo (Figure 6), and SAPK-1s are not involved in the arsenite-induced phosphorylation. The involvement of these enzymes was ascertained by overexpression of SAPK-1γ in the presence of arsenite (Figure 6). Overexpression of SAPK-1γ and activation by arsenite, as demonstrated by the phosphorylation of its activation domain, only marginally increased AT270 and PHF-1 immunoreactivity (Figure 6), and no increase was observed for AT8 and PHF-6 (data not shown). Overexpression of active SAPK-1γ by infecting with SFV/SAPK-1γ/SAPKK-1 also did not result in *tau* phosphorylation. These results, for the most part, are consistent with a recent study demonstrating that *tau* is a poor substrate for SAPK-1γ in vivo, although it also was shown that when overexpressed SAPK-1γ may modify the AT270 epitope (*89*).

Likewise SAPK-2s are not involved in steady state or arsenite-induced phosphorylation of *tau* in CHO T40 cells (Figure 1A). Buee-Scherrer and Goedert (*89*) recently showed that SAPK-2α can phosphorylate *tau* in COS 7 cells under conditions of overexpression and osmotic stress. Other MAPKs, SAPK-4 and ERK-5, have previously been shown not to phosphorylate *tau* in vivo (*72*); however, Buee-Scherrer and Goedert (*89*) demonstrated that, when overexpressed, SAPK-4 may phosphorylate *tau*. SAPK-3 overexpression can result in an increase in phosphorylation of *tau* (*72*, *89*), but it is unlikely that SAPK-3 is involved in *tau* phosphorylation in either CHO cells or in neurons, since it is predominantly expressed in skeletal muscle (*20*, *22*, *23*).

Analysis of cells in interphase versus mitosis (Figure 7), as well as data from the protein kinase inhibitors (Figure 8A), demonstrate that the activity involved in the arsenite-induced phosphorylation of *tau* is not a cyclin-dependent kinase, including cdk5. Consistent with this notion, using an immunoprecipitation kinase assay (*93*), it was not possible to detect any cdk5 activity in untreated or arsenite-treated CHO cells (data not shown). Expression of p35, the major activator of cdk5, was also below detectable levels in these cells (data not shown). It is thought that cdk5 is a major modifier of *tau in vivo*, but it is not required for arsenite-induced phosphorylation of *tau* in cultured cells. Phosphorylation by cdk5, however, may be additive to that of the kinases activated by arsenite in promoting the hyperphosphorylation of *tau* in neurons. It is also possible that arsenite may have an effect on cdk5 activity, but this remains to be evaluated. A caveat of using cells devoid of cdk5 is that this system may not fully represent the phosphorylation state of *tau* in adult neurons. This system nevertheless allows the demonstration that extensive *tau* phosphorylation can occur in living cells without active cdk5.

Inhibition of the major PPs that typically regulate *tau* phosphorylation also does not seem to be a factor, and in fact, the effects of arsenite are much greater than those seen following the inhibition of PP-1 and -2A (Figure 8B). The kinase(s) involved in arsenite-induced phosphorylation remains elusive, but the inhibition by roscovitine of all phosphorylation sites specifically monitored with antibodies (Figures 8A and 10) suggests that it may be a single kinase or a single family of kinases. The ability to reconstitute *tau* phosphorylation activity(ies) in cell extracts and its inhibition with roscovitine further indicates that the effect of arsenite on *tau* phosphorylation is due to kinase activation. Furthermore, it is likely that this activity may eventually be purified biochemically.

Jenkins and Johnson (*91*, *92*) had previously demonstrated that the arsenic-containing compound PAO could induce the phosphorylation of *tau* in cultures cells at the 12E8 epitope. Since arsenite and PAO may have similar effects on cells, the outcome of both agents on *tau* phosphorylation was compared. PAO had a similar effect in increasing *tau* phosphorylation at all the sites monitored, albeit the increase was more modest (Figure 10). The increase in phosphorylation at Ser-262/Ser-356 in *tau* in SH-SY5Y cells following PAO exposure has been attributed to an increase in MARK activity, since both the increased phosphorylation and increased MARK activity were inhibited by the kinase inhibitor staurosporine (*92*). However, in CHO T40 cells treated with arsenite, no increase in MARK activity could be detected by in-gel kinase assay (Figure 9A). This disparity could be due to differences in the signal transduction pathways between each cell line, or differences in the ability of arsenite or PAO to activate MARK. Nevertheless, this result and the lack of an inhibition by staurosporine (Figure 11) indicate that MARK does not play a significant role in increased *tau* phosphorylation induced by arsenite in CHO T40 cells. This notion is also consistent with MARK being a nonproline directed kinase that predominantly modifies Ser-262/Ser-356 in *tau* (*85*), but not the proline-directed sites that are also phosphorylated following arsenite exposure. The kinase(s) involved are likely to be members of the expanding family of stress-inducible/proline-directed kinases. Interestingly, under specific conditions some proline-directed kinases can also phosphorylate non-proline-directed sites such as Ser-262/Ser-356 in *tau* (*94*). Importantly, the arsenite-inducible kinase activity is expressed in several different cell lines, including CHO cells, HEK 293 cells and the neuronal cell line Neuro 2A (Figure 12), suggesting that it may have a more general function.

The discovery of mutations in the *tau* gene has directly linked aberrations in *tau* to neurodegenerative diseases. Some of these mutations affect *tau* mRNA splicing, but missense mutations can also cause disease [reviewed in ref *3*]. In vitro reduction in microtubule binding and the impairment of the

ability to promote microtubule assembly are the most commonly reported consequences of missense mutations, but acceleration in the rate of fibrillization may also be important (*73*). Furthermore, missense mutations may have long-range effects on the phosphorylation of *tau* in vitro (*67*). The effect of *tau* mutations on arsenite-induced phosphorylation was investigated in stably transfected CHO cells (Figure 13). Arsenite results in increased modification of the PHF-1 and AT270 epitopes in wild-type and single mutant *tau* proteins. The artificial triple mutant VPR exhibited increased immunoreactivity of the PHF-1 epitope, and a significant increase in overall phosphorylation was observed by a decrease in gel mobility, but there was no increase in the phosphorylation of Ser-181 (i.e., AT270 phosphoepitope). Some mutant proteins had higher basal phosphorylation of Ser-231 than wild-type *tau*, but arsenite did not increase the phosphorylation of Ser-231 (i.e., PHF-6 immunoreactivity) in any of the mutant proteins, while there was a pronounced increase for the wild-type protein. The R406W mutation had the greatest impact in reducing the phosphorylation of Ser-231 under normal conditions as well as arsenite stress, and it also reduced the extent of phosphorylation at the PHF-1 and AT270 epitopes resulting from arsenite exposure. These results demonstrate that mutations in *tau* can affect properties of the protein distant from the site of the mutations. These differences in phosphorylation patterns demonstrate that the mutations must cause significant structural changes in vivo. The complexity and long-range effects of single amino acid substitutions underscore the difficulty in monitoring and predicting changes in protein structure in live cells.

The mechanism of PHF-*tau* formation in neurons is still enigmatic, but aberrant hyperphosphorylation has been proposed as a possible mechanism. Hyperphosphorylation greatly increases the propensity of *tau* to polymerize into fibrils in vitro (*74*). In addition, phosphorylation inhibits microtubule binding (*54*, *75*, *76*), and the impaired ability of PHF-*tau* to bind to microtubules can be overcome by dephosphorylation (*77*). PHF formation may be promoted by the reduced affinity of hyperphosphorylated *tau* for microtubules, resulting in a higher level of unbound *tau*, which may aggregate to form PHFs. The importance of phosphorylation in the formation of *tau* polymers is further supported by the finding that hyperphosphorylation of *tau* precedes PHF formation (*78*, *79*). A possible scenario for the demise of neurons in AD and other diseases associated with PHF formation may involve chronic or perhaps repetitive acute insults to neurons leading to activation of signal cascades. The ensuing hyperphosphorylation of *tau* may result in microtubule destabilization and dysfunction. This could constitute a secondary insult to neuronal integrity that could result in further activation of *tau* kinase(s). Under certain conditions, a threshold imbalance of kinase activity over phosphatase activity may be reached, such that neurons may enter a self-perpetuating cycle, resulting in chronic elevation of kinase activity and an increase in the pool of unbound hyperphosphorylated *tau* available for PHF formation. Perhaps the aging nervous system, being less capable of coping with stresses, is more easily pushed over the threshold that leads to PHF formation. Genetic factors may also affect the cellular ability to handle insults and alter selective vulnerability.

We are not aware of any reports exploring a link between arsenite exposure and Alzheimer's disease or any late-onset neurodegenerative diseases. The lack of epidemiological studies may be due to the notion that arsenite does not readily cross the blood-brain barrier, but recently it was shown that arsenite can accumulate in the brain where it affects functionally important parameters such as levels of neurotransmitters (*80*, *81*). Furthermore, recently it has been demonstrated that *tau* phosphorylation is affected by physiological stresses. For example, in mice, starvation can induce *tau* hyperphosphorylation with a spatial distribution reminiscent of *tau* distribution in AD brain (i.e., hippocampus > cortex > cerebellum) (*82*). These results suggest that environmental and physiological stress, perhaps including amyloid plaque accumulation or other heavy metals, that may have a similar impact as arsenite may have a prominent role in the etiology of AD. Further studies focused on delineating the signal cascades and environmental factors involved could lead to preventative and therapeutic strategies.

ACKNOWLEDGMENT

The authors would like to thank Dr. P. Davies for the antibody PHF-1, Dr. R. Davies for the Flag-SAPK-1γ construct, and Dr. M. Karin for the human HA-SAPK-1γ and SAPKK-1 cDNAs.

REFERENCES

1. Spillantini, M. G., and Goedert, M. (1998) *Trends Neurosci. 21*, 428−433.
2. Trojanowski, J. Q., and Lee, V. M.-Y. (2000) *Ann. N.Y. Acad. Sci. 924*, 62−67.
3. Forman, M. S., Lee, V. M.-Y., and Trojanowski, J. Q. (2000) *J. Chem. Neuroanat. 20*, 225−244.
4. Morishima-Kawashima, M., Hasegawa, M., Takio, K., Suzuki, M., Yoshida, H., Titani, K., and Ihara, Y. (1995) *J. Biol. Chem. 270*, 823−829.
5. Hanger, D. P., Betts, J. C., Loviny, T. L., Blackstock, W. P., and Anderton, B. H. (1998) *J. Neurochem. 71*, 2465−2476.
6. Billingsley, M. L. and Kincaid, R. L. (1997) *Biochem. J. 323* (*Pt 3*), 577−591.
7. Reynolds, C. H., Nebreda, A. R., Gibb, G. M., Utton, M. A., and Anderton, B. H. (1997) *J. Neurochem. 69*, 191−198.
8. Reynolds, C. H., Utton, M. A., Gibb, G. M., Yates, A., and Anderton, B. H. (1997) *J. Neurochem. 68*, 1736−1744.
9. Goedert, M., Hasegawa, M., Jakes, R., Lawler, S., Cuenda, A., and Cohen, P. (1997) *FEBS Lett. 409*, 57−62.
10. Cano, E., and Mahadevan, L. C. (1995) *Trends Biochem. Sci. 20*, 117−122.
11. Minden, A., and Karin, M. (1997) *Biochim. Biophys. Acta 1333*, F85−104.
12. Boulton, T. G., Nye, S. H., Robbins, D. J., Ip, N. Y., Radziejewska, E., Morgenbesser, S. D., DePinho, R. A., Panayotatos, N., Cobb, M. H., and Yancopoulos, G. D. (1991) *Cell 65*, 663−675.
13. Zhou, G., Bao, Z. Q., and Dixon, J. E. (1995) *J. Biol. Chem. 270*, 12665−12669.
14. Gupta, S., Barrett, T., Whitmarsh, A. J., Cavanagh, J., Sluss, H. K., Derijard, B., and Davis, R. J. (1996) *EMBO J. 15*, 2760−2770.
15. Kyriakis, J. M., Banerjee, P., Nikolakaki, E., Dai, T., Rubie, E. A., Ahmad, M. F., Avruch, J., and Woodgett, J. R. (1994) *Nature 369*, 156−160.
16. Lee, J. C., Laydon, J. T., McDonnell, P. C., Gallagher, T. F., Kumar, S., Green, D., McNulty, D., Blumenthal, M. J., Heys, J. R., and Landvatter, S. W. (1994) *Nature 372*, 739−746.
17. Han, J., Lee, J. D., Bibbs, L., and Ulevitch, R. J. (1994) *Science 265*, 808−811.
18. Enslen, H., Raingeaud, J., and Davis, R. J. (1998) *J. Biol. Chem. 273*, 1741−1748.

19. Stein, B., Yang, M. X., Young, D. B., Janknecht, R., Hunter, T., Murray, B. W., and Barbosa, M. S. (1997) *J. Biol. Chem. 272*, 19509−19517.
20. Li, Z., Jiang, Y., Ulevitch, R. J., and Han, J. (1996) *Biochem. Biophys. Res. Commun. 228*, 334−340.
21. Mertens, S., Craxton, M., and Goedert, M. (1996) *FEBS Lett. 383*, 273−276.
22. Lechner, C., Zahalka, M. A., Giot, J. F., Moller, N. P., and Ullrich, A. (1996) *Proc. Natl. Acad. Sci. U.S.A. 93*, 4355−4359.
23. Wang, X. S., Diener, K., Manthey, C. L., Wang, S., Rosenzweig, B., Bray, J., Delaney, J., Cole, C. N., Chan-Hui, P. Y., Mantlo, N., Lichenstein, H. S., Zukowski, M., and Yao, Z. (1997) *J. Biol. Chem. 272*, 23668−23674.
24. Jiang, Y., Gram, H., Zhao, M., New, L., Gu, J., Feng, L., Di Padova, F., Ulevitch, R. J., and Han, J. (1997) *J. Biol. Chem. 272*, 30122−30128.
25. Goedert, M., Cuenda, A., Craxton, M., Jakes, R., and Cohen, P. (1997) *EMBO J. 16*, 3563−3571.
26. Subcommittee on arsenite in drinking water, N. R. C. U. S. (1999) in *Arsenic in drinking water*. National Academy Press, Washington, DC.
27. Ayres, R. U. (1992) *Proc. Natl. Acad. Sci. U. S.A 89*, 815−820.
28. Snow, E. T. (1992) *Pharm. Ther. 53*, 31−65.
29. Gorby, M. S. (1994) in *Arsenic in the Environment* (Nriagu, J. O., Ed.) pp 1−16, John Wiley & Sons, Inc., New York.
30. Morton, W. E., and Dunnette, D. A. (1994) in *Arsenic in the Environment* (Nriagu, J. O., Ed.) pp 17−34, John Wiley & Sons, Inc, New York.
31. Jenkins, R. B. (1966) *Brain 89*, 479−498.
32. Goebel, H. H., Schmidt, P. F., Bohl, J., Tettenborn, B., Kramer, G., and Gutmann, L. (1990) *J. Neuropathol. Exp. Neurol. 49*, 137−149.
33. Le Quesne, P. M., and McLeod, J. G. (1977) *J. Neurol. Sci. 32*, 437−451.
34. Greenberg, C., Davies, S., McGowan, T., Schorer, A., and Drage, C. (1979) *Chest 76*, 596−598.
35. Freeman, J. W., and Couch, J. R. (1978) *Neurology 28*, 853−855.
36. Fincher, R. M., and Koerker, R. M. (1987) *Am. J. Med. 82*, 549−552.
37. O'Shaughnessy, E., and Kraft, G. H. (1976) *Arch. Phys. Med. Rehabil. 57*, 403−406.
38. Morton, W. E., and Caron, G. A. (1989) *Am. J. Ind. Med. 15*, 1−5.
39. Danan, M., Dally, S., and Conso, F. (1984) *Neurology 34*, 1524.
40. Abernathy, C. O., Liu, Y. P., Longfellow, D., Aposhian, H. V., Beck, B., Fowler, B., Goyer, R., Menzer, R., Rossman, T., Thompson, C., and Waalkes, M. (1999) *Environ. Health Perspect. 107*, 593−597.
41. Liu, S. X., Athar, M., Lippai, I., Waldren, C., and Hei, T. K. (2001) *Proc. Natl. Acad. Sci. U.S.A. 98*, 1643−1648.
42. Delnomdedieu, M., Basti, M. M., Otvos, J. D., and Thomas, D. J. (1993) *Chem. Res. Toxicol. 6*, 598−602.
43. Kato, K., Ito, H., and Okamoto, K. (1997) *Cell Stress. Chaperones. 2*, 199−209.
44. Liu, Y., Guyton, K. Z., Gorospe, M., Xu, Q., Lee, J. C., and Holbrook, N. J. (1996) *Free Radic. Biol. Med. 21*, 771−781.
45. Giasson, B. I., and Mushynski, W. E. (1996) *J. Biol. Chem. 271*, 30404−30409.
46. Sperber, B. R., Leight, S., Goedert, M., and Lee, V. M.-Y. (1995) *Neurosci. Lett. 197*, 149−153.
47. Goedert, M., Spillantini, M. G., Jakes, R., Rutherford, D., and Crowther, R. A. (1989) *Neuron 3*, 519−526.
48. Vogelsberg-Ragaglia, V., Bruce, J., Richter-Landsberg, C., Zhang, B., Hong, M., Trojanowski, J. Q., and Lee, V. M.-Y. (2000) *Mol. Biol. Cell 11*, 4093−4104.
49. Illenberger, S., Zheng-Fischhofer, Q., Preuss, U., Stamer, K., Baumann, K., Trinczek, B., Biernat, J., Godemann, R., Mandelkow, E. M., and Mandelkow, E. (1998) *Mol. Biol. Cell 9*, 1495−1512.
50. Sihag, R. K., and Nixon, R. A. (1990) *J. Biol. Chem. 265*, 4166−4171.
51. Rolls, M. M., Haglund, K., and Rose, J. K. (1996) *Virology 218*, 406−411.
52. Liljestrom, P., and Garoff, H. (1991) *Biotechnology (N.Y.) 9*, 1356−1361.
53. Lee, V. M.-Y., Balin, B. J., Otvos, L., Jr., and Trojanowski, J. Q. (1991) *Science 251*, 675−678.
54. Lindwall, G., and Cole, R. D. (1984) *J. Biol. Chem. 259*, 5301−5305.
55. Otvos, L., Jr., Feiner, L., Lang, E., Szendrei, G. I., Goedert, M., and Lee, V. M.-Y. (1994) *J. Neurosci. Res. 39*, 669−673.
56. Hoffmann, R., Lee, V. M.-Y., Leight, S., Varga, I., and Otvos, L., Jr. (1997) *Biochemistry 36*, 8114−8124.
57. Goedert, M., Jakes, R., and Vanmechelen, E. (1995) *Neurosci. Lett. 189*, 167−169.
58. Goedert, M., Jakes, R., Crowther, R. A., Cohen, P., Vanmechelen, E., Vandermeeren, M., and Cras, P. (1994) *Biochem. J. 301 (Pt 3)*, 871−877.
59. Cuenda, A., Rouse, J., Doza, Y. N., Meier, R., Cohen, P., Gallagher, T. F., Young, P. R., and Lee, J. C. (1995) *FEBS Lett. 364*, 229−233.
60. Favata, M. F., Horiuchi, K. Y., Manos, E. J., Daulerio, A. J., Stradley, D. A., Feeser, W. S., Van Dyk, D. E., Pitts, W. J., Earl, R. A., Hobbs, F., Copeland, R. A., Magolda, R. L., Scherle, P. A., and Trzaskos, J. M. (1998) *J. Biol. Chem. 273*, 18623−18632.
61. Hong, M., Chen, D. C., Klein, P. S., and Lee, V. M.-Y. (1997) *J. Biol. Chem. 272*, 25326−25332.
62. Vega, L., Gonsebatt, M. E., and Ostrosky-Wegman, P. (1995) *Mutat. Res. 334*, 365−373.
63. Huang, S. C., and Lee, T. C. (1998) *Carcinogenesis 19*, 889−896.
64. Li, Y. M., and Broome, J. D. (1999) *Cancer Res. 59*, 776−780.
65. Preuss, U., Doring, F., Illenberger, S., and Mandelkow, E. M. (1995) *Mol. Biol. Cell 6*, 1397−1410.
66. Hong, M., Zhukareva, V., Vogelsberg-Ragaglia, V., Wszolek, Z., Reed, L., Miller, B. I., Geschwind, D. H., Bird, T. D., McKeel, D., Goate, A., Morris, J. C., Wilhelmsen, K. C., Schellenberg, G. D., Trojanowski, J. Q., and Lee, V. M.-Y. (1998) *Science 282*, 1914−1917.
67. Connell, J. W., Gibb, G. M., Betts, J. C., Blackstock, W. P., Gallo, J., Lovestone, S., Hutton, M., and Anderton, B. H. (2001) *FEBS Lett. 493*, 40−44.
68. Drewes, G., Lichtenberg-Kraag, B., Doring, F., Mandelkow, E. M., Biernat, J., Goris, J., Doree, M., and Mandelkow, E. (1992) *EMBO J. 11*, 2131−2138.
69. Roder, H. M., Eden, P. A., and Ingram, V. M. (1993) *Biochem. Biophys. Res. Commun. 193*, 639−647.
70. Lovestone, S., Reynolds, C. H., Latimer, D., Davis, D. R., Anderton, B. H., Gallo, J. M., Hanger, D., Mulot, S., Marquardt, B., Stabel, S., Woodgett, J. R., and Miller, C. C. J. (1994) *Curr. Biol. 4*, 1077−1086.
71. Latimer, D. A., Gallo, J. M., Lovestone, S., Miller, C. C., Reynolds, C. H., Marquardt, B., Stabel, S., Woodgett, J. R., and Anderton, B. H. (1995) *FEBS Lett. 365*, 42−46.
72. Jenkins, S. M., Zinnerman, M., Garner, C., and Johnson, G. V. (2000) *Biochem. J. 345 Pt 2*, 263−270.
73. Goedert, M., Jakes, R., and Crowther, R. A. (1999) *FEBS Lett. 450*, 306−311.
74. Alonso, A. C., Zaidi, T., Novak, M., Grundke-Iqbal, I., and Iqbal, K. (2001) *Proc. Natl. Acad. Sci. U.S.A. 98*, 6923−6928.
75. Drechsel, D. N., Hyman, A. A., Cobb, M. H., and Kirschner, M. W. (1992) *Mol. Biol. Cell 3*, 1141−1154.
76. Gustke, N., Steiner, B., Mandelkow, E. M., Biernat, J., Meyer, H. E., Goedert, M., and Mandelkow, E. (1992) *FEBS Lett. 307*, 199−205.
77. Bramblett, G. T., Goedert, M., Jakes, R., Merrick, S. E., Trojanowski, J. Q., and Lee, V. M.-Y. (1993) *Neuron 10*, 1089−1099.
78. Braak, E., Braak, H., and Mandelkow, E. M. (1994) *Acta Neuropathol. (Berl) 87*, 554−567.
79. Yoshida, H. and Ihara, Y. (1993) *J. Neurochem. 61*, 1183−1186.
80. Delgado, J. M., Dufour, L., Grimaldo, J. I., Carrizales, L., Rodriguez, V. M., and Jimenez-Capdeville, M. E. (2000) *Toxicol. Lett. 117*, 61−67.
81. Biswas, U., Sarkar, S., Bhowmik, M. K., Samanta, A. K., and Biswas, S. (2000) *Small Ruminant Res. 38*, 229−235.
82. Yanagisawa, M., Planel, E., Ishiguro, K., and Fujita, S. C. (1999) *FEBS Lett. 461*, 329−333.
83. Cohen, P., Klumpp, S., and Schelling, D. L. (1989) *FEB Lett. 250*, 596−600.
84. Ishihara, H., Martin, B. L., Brautigan, D. L., Karaki, H., Ozaki, H., Kata, Y., Fusetani, N., Watabe, S., Hashimoto, K., Uemura, D., Hartshorne, D. J. (1989) *Biochem. Biophys. Res. Commun. 159*, 871−877.

85. Drewes, G., Ebneth, A., Preuss, U., Mandelkow, E.-M., Mandelkow, E. (1997) *Cell 89*, 297−308.
86. Meijer, L., Borgne, A., Mulner, O., Chong, J. P. J., Blow, J. J. Inagaka, N., Inagaki, M., Delcros, J.-G., and Moulinous, J.-P. (1997) *Eur. J. Biochem. 243*, 527−536.
87. Leost, M., Schultz, C., Link, A., Wu, Y.-Z., Biernat, J., Mandelkow, E.-M., Bibb, J. A., Snyder, G. L., Greengard, P., Zaharevitz, D. W., Gussio, R., Senderowicz, A. M., Sausville, E. A., Kunick, C., and Meijer, L. (2000) *Eur. J. Biochem. 267*, 5983−5994.
88. Zaharevitz, D. W., Gussio, R., Leost, M., Senderowicz, A. M., Lahusen, T., Kunick, C., Meijer, L., and Sausville, E. A. (1999) *Cancer Res. 59*, 2566−2569.
89. Buee-Scherrer, V., and Goedert, M. (2002) *FEBS Lett. 515*, 151−154.
90. Seubert, P., Mawal-Dewan, M., Barbour, R., Jakes, R., Goedert, M., Johnson, G. V. W., Litersky, J. M., Schenk, D., Lieberburg, I., Trojanowski, J. Q., and Lee, V. M.-Y. (1995) *J. Biol. Chem. 270*, 18917−18922.
91. Jenkins, S. M., and Johnson, G. V. W. (1999) *J. Neurochem. 73*, 1843−1850.
92. Jenkins, S. M., and Johnson, G. V. W. (2000) *J. Neurochem. 74*, 1463−1468.
93. Giasson, B. I., and Mushynski, W. E. (1997) *J. Neurosci. 17*, 9466−9472.
94. Hasegawa, M., Crowther, R. A., Jakes, R., and Goedert, M. (1997) *J. Biol. Chem. 272*, 33118−33124.
95. Namguang, U., and Xia, Z. (2000) *J. Neurosci. 20*, 6442−6451.

BI026813C